

RADIATIVE PRODUCTION OF THE $\Lambda(1405)$ RESONANCE IN K^- COLLISIONS ON PROTONS AND NUCLEI

J.C. Nacher^{1,2}, E. Oset^{1,2}, H. Toki¹ and A. Ramos³

¹ *Research Center for Nuclear Physics (RCNP), Osaka University, Ibaraki, Osaka 567-0047, Japan.*

² *Departamento de Física Teórica and IFIC, Centro Mixto Universidad de Valencia-CSIC 46100 Burjassot (Valencia), Spain.*

³ *Departament d'Estructura i Constituents de la Materia, Universitat de Barcelona, Diagonal 647, 08028 Barcelona, Spain.*

Abstract

We have carried a theoretical study of the $K^-p \rightarrow MB\gamma$ reaction with $MB = K^-p, \bar{K}^0n, \pi^-\Sigma^+, \pi^+\Sigma^-, \pi^0\Sigma^0, \pi^0\Lambda$, for K^- lab. momenta between 200 and 500 MeV/c, using a chiral unitary approach for the strong K^-p interaction with its coupled channels. The $\Lambda(1405)$ resonance, which is generated dynamically in this approach, shows up clearly in the $d\sigma/dM_I$ spectrum, providing new tests for chiral symmetry and the unitary approach, as well as information regarding the nature of the resonance. The photon detection alone, summing all channels, is shown to reproduce quite accurately the strength and shape of the $\Lambda(1405)$ resonance. Analogous reactions in nuclei can provide much information on the properties of this resonance in a nuclear medium.

The $\Lambda(1405)$ resonance, S_{01} , $I(J^P)=0(\frac{1}{2}^-)$, appears just below the K^-p threshold and plays an essential role in the K^-p interaction and coupled channels at low energies. The modification of its properties in nuclei influences directly the K^- nucleus interaction, a topic which has raised much theoretical interest [1, 2, 3] in order to explain the attraction manifested by empirical analyses of K^- atoms [4] and which eventually could lead to K^- condensation in neutron stars [5].

Another attractive feature of the $\Lambda(1405)$ resonance is its dynamical generation within the context of chiral unitary theories [6, 7, 8] which lead to a good description of the low energy $\bar{K}N$ interaction and coupled channels. The dynamical generation of the $\Lambda(1405)$ in the chiral context has larger repercussion than just the description of these strong interactions in the strangeness $S = -1$ sector. It also leads to define mechanisms for its electromagnetic production or decay. The strength of these mechanisms also changes from one reaction to another and as a function of the energy. Hence, the investigation of these reactions offers a test of chiral symmetry and of the nonperturbative methods used to generate the low lying resonances. One such test, which is passed successfully, is offered by the $K^-p \rightarrow \Lambda\gamma, \Sigma^0\gamma$ reaction, where the unitarity in coupled channels enhances the $\Sigma^0\gamma$ production by more than one order of magnitude [9]. Photoproduction processes in the $S = 0$ sector within the chiral schemes have equally proved successful [7].

In a recent paper [10] a study of the $\Lambda(1405)$ photoproduction process close to threshold was done in the $\gamma p \rightarrow K^+\Lambda(1405)$ reaction, showing that the K^+ detection alone was a good tool to observe the resonance. This reaction, implemented in nuclei, was already suggested in [1] as a means to observe modifications of the $\Lambda(1405)$ resonance in a nuclear medium. In [10] was shown that the study of the resonance in nuclei required the specific detection of the $\pi\Sigma$ decay channels of the $\Lambda(1405)$, the Fermi motion blurring any trace of the resonance if only the K^+ is detected.

In the present paper we study a crossed channel of the former reaction, namely the $K^-p \rightarrow \Lambda(1405)\gamma$ reaction at low K^- energies. One novelty of the present reaction is that the photon has now small energy, of the order of 100 MeV in the energy regime studied here, while the photon required in the $\gamma p \rightarrow K^+\Lambda(1405)$ reaction had around 1.7 GeV. The smaller energy of the K^- and γ in the $K^-p \rightarrow \Lambda(1405)\gamma$ reaction makes the effects of Fermi motion in nuclei much weaker, such that the detection of the photon still leads to a resonant shape in the cross section. Another novelty is that the reactions are rather different dynamically, with the dominant mechanisms in the first reaction being negligible in the second one, and others which could be proved negligible in the first one becoming now dominant in the second reaction. Hence, in spite of the similarities of the two reactions, the information provided by them as tests of the chiral approaches are different and complementary.

We shall follow the chiral approach of [8] for the strong interaction in the $S = -1$ sector where the Bethe Salpeter [BS] equation is solved with the coupled channels $K^-p, \bar{K}^0n, \pi^0\Lambda, \pi^0\Sigma^0, \eta\Lambda, \eta\Sigma^0, \pi^+\Sigma^-, \pi^-\Sigma^+, K^+\Xi^-, K^0\Xi^0$.

The BS equation reads in matrix form:

$$T = V + VGT \rightarrow T = [1 - VG]^{-1}V, \quad (1)$$

with G a diagonal matrix, accounting for a loop with a meson and a baryon propagator, with matrix elements

$$G_l(s) = i \int \frac{d^4 q_L}{(2\pi)^4} \frac{M_l}{E_l(\vec{q}_L)} \frac{1}{\sqrt{s} - q_L^0 - E_l(\vec{q}_L) + i\epsilon} \frac{1}{q_L^2 - m_l^2 + i\epsilon} \quad (2)$$

and V is the transition matrix extracted from the lowest order chiral Lagrangian, which in the s-wave and usual low energy approximation reads as [8]

$$V_{ij} = -C_{ij} \frac{1}{4f^2} (k^0 + k'^0), \quad (3)$$

where k, k' are the momenta of the incoming, outgoing mesons, f is the pion decay constant ($f_\pi = 93$ MeV) and C_{ij} a 10×10 matrix of coefficients which are shown in table 1 of [8]. In [8] an average value $f = 1.15f_\pi$, between the one for pions and kaons is used. This, together with the choice of a cut off, $|\vec{q}_L|_{max}$, in the integral of eq. (2), provides an effective way of accounting for effects of the higher order Lagrangians in this particular sector (see ref. [11] for an interpretation within the more general inverse amplitude method). Eq. (1) is an algebraic equation, and the loop integral affects only the meson and baryon propagators in G_l , since it was proved in [8] that V and T factorized outside the integral with their on shell values.

The series of diagrams summed up by the BS equation is shown in line (1) of fig 1. From there we can draw all diagrams in which an external photon is coupled in addition, which leads to the rest of diagrams shown in the figure.

Apart from the strong $MB \rightarrow M'B'$ vertices of eq. (3) we need now the coupling of the photon to the baryons, the mesons, plus the contact term of diagram (2,a) of fig. 1 required by gauge invariance. These vertices are standard and after the nonrelativistic reduction of the γ matrices, are given in the Coulomb gauge, $\epsilon^0 = 0$, $\vec{\epsilon} \cdot \vec{q} = 0$, with \vec{q} the photon momentum, by

$$a) -it_{M'M\gamma} = 2ieQ_M \vec{k}' \cdot \vec{\epsilon} \quad (4)$$

for the coupling of the photon to the mesons, with e electron charge, Q_M the charge of the meson, k' the momentum of the outgoing meson and ϵ_μ the photon polarization vector.

$$b) -it_{B'B\gamma} = ie(Q_B \frac{\vec{p} + \vec{p}'}{2M_B} - i \frac{\vec{\sigma} \times \vec{q}}{2M_B} \mu_B) \vec{\epsilon} \quad (5)$$

for the coupling of the photon to the baryons, with Q_B the baryon charges, \vec{p}, \vec{p}' incoming and outgoing momenta of the baryon and M_B, μ_B the mass and the magnetic moment of the baryon.

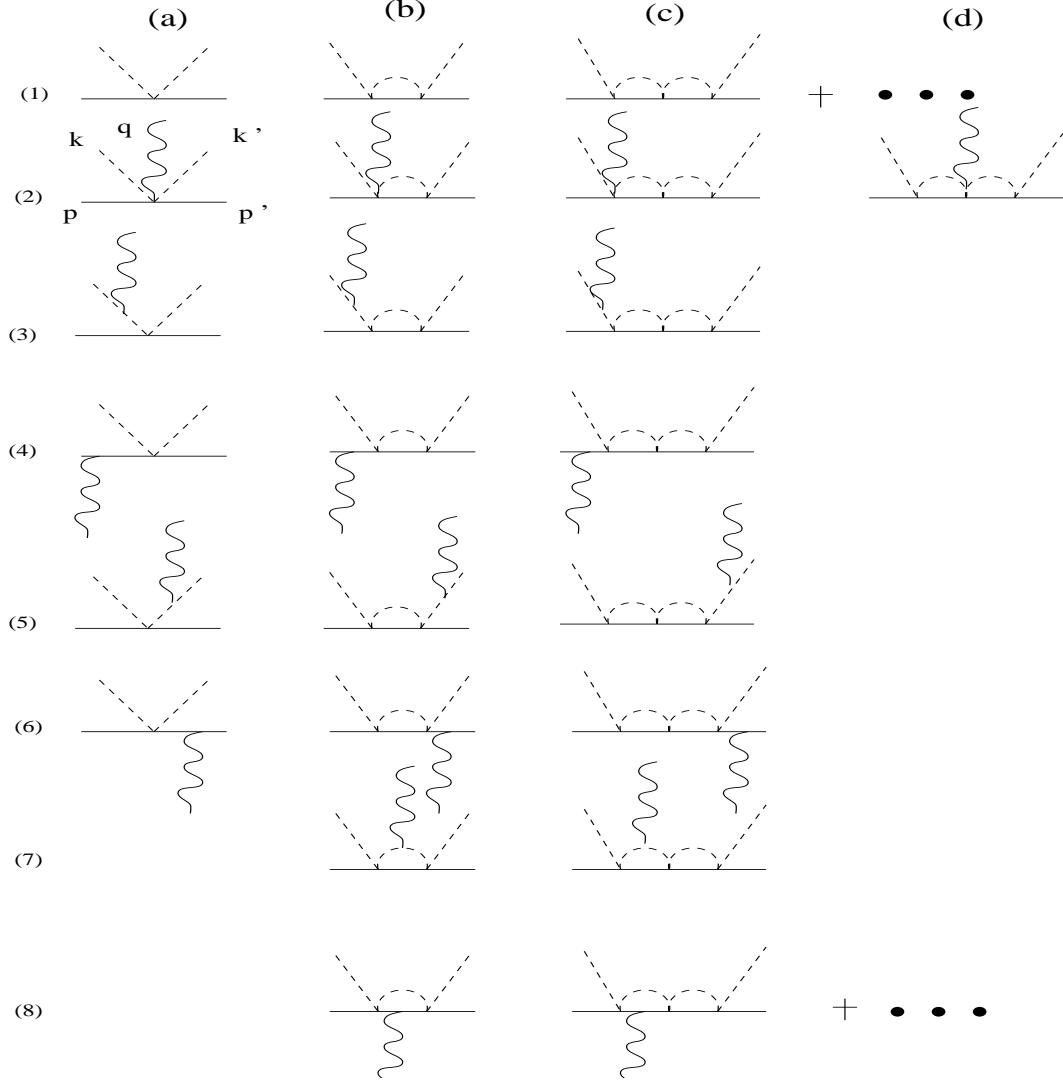


Figure 1: Feynman diagrams used in the model for the $K^- p \rightarrow \Lambda(1405)\gamma$ reaction.

$$c) - it_{B'M'BM\gamma} = iC_{ij}(Q_i + Q_j)\left\{\frac{\vec{p} + \vec{p}'}{2M} - i\frac{\vec{\sigma} \times (\vec{p} - \vec{p}')}{2M}\right\}\vec{\epsilon} \quad (6)$$

for the contact term of diagram (2,a) of fig. 1, with C_{ij} the coefficients of eq. (3), i, j standing for a BM state, Q_i, Q_j the charges of the mesons, \bar{M} an average mass of the baryons and \vec{p}, \vec{p}' the momenta of the incoming and outgoing baryons.

We shall be concerned with K^- with momenta below 500 MeV/c in the lab frame. In this energy domain it is easy to see that the Bremsstrahlung diagrams from mesons and baryons (diagrams (3,a)(4,a)(5,a)(6,a)) are of the same order of magnitude and that the contact term (diagram (2,a)) is of order $q/2M$ of the corresponding meson Bremsstrahlung diagrams ((3,a) and (5,a)). With CM photon momenta q of the order of 150 MeV or below, these terms

represent corrections below the 8% level and we shall neglect them. In addition, terms like in diagram (2,d), where the photon couples to internal vertices of the loops, vanish for parity reasons.

The diagrams of row (7) of fig. 1 where the photon couples to mesons in the loops vanish due to the gauge condition $\vec{\epsilon} \cdot \vec{q} = 0$ and the same happens to the diagrams in row (8) where the photon couples with the dielectric part $((\vec{p} + \vec{p}'))$ term of eq. (5)) to the baryons inside the loops. This occurs because in both cases one has integrals of the type $\vec{\epsilon} \int d^3k \vec{k} \cdot f(k, q)$ and the integral gives a vector proportional to \vec{q} , the only vector in the integrand which is not integrated when we work in the CM frame. The magnetic coupling of the photons in row (8) survives.

Hence, the process is given, within the approximations mentioned, by the diagrams of the rows 3, 4, 5, 6 plus the magnetic part in row 8. This situation is opposite to the one found in [10] for $\Lambda(1405)$ photoproduction close to threshold, where the dominant terms came from the contact term and the Bremsstrahlung diagrams were negligible.

If we inspect the series of terms in rows (3) and (4) of fig. 1 we see that the strong part of the interaction to the right of the electromagnetic vertex involves the sum $V + VGV + \dots = V + VGT$. This is the T matrix from the initial MB state to the final $M'B'$ state after losing the energy of the photon, this is, with an argument M_I , where M_I is the invariant mass of the $M'B'$ state. Similarly, in the rows (5) (6) the strong T matrix factorizes before the electromagnetic vertex with an argument \sqrt{s} , with s the Mandelstam variable for the initial K^-p system. In the diagrams of row (8) we have a loop with one meson and two baryons. The strong interaction to the left originates $t(\sqrt{s})$ and the one to the right $t(M_I)$. In order to evaluate the loop function we note that $q \ll \omega(q_L)$ and neglecting q in the second baryon propagator we observe that the baryon propagator appears squared and hence this loop function can be obtained by differentiation of the loop of eq. (2) with respect to \sqrt{s} , which is what we do. This term gives a contribution of less than 10% in the cross section and this approximation is hence justified.

Thus, a straightforward calculation, which includes the vertices of eqs.(4, 5), plus the meson and baryon propagators, allows one to write the whole amplitude for the process in terms of an electric and a magnetic part as:

$$t_{ij}^{(\gamma)} = t_{ij}^{(1E)} \vec{k} \cdot \vec{\epsilon} + t_{ij}^{(2E)} \vec{k}' \cdot \vec{\epsilon} + it^{(M)} (\vec{\sigma} \times \vec{q}) \cdot \vec{\epsilon}, \quad (7)$$

where

$$t_{ij}^{(1E)} = eQ_i \left(\frac{1}{k \cdot q} + \frac{1}{qM_i} \right) t_{ij}(M_I), \quad (8)$$

$$t_{ij}^{(2E)} = -eQ_j \left(\frac{1}{k' \cdot q} + \frac{1}{qM_j} \right) t_{ij}(\sqrt{s}), \quad (9)$$

$$t^{(M)} = -\frac{e\mu_{Bi}}{2qM_i} t_{ij}(M_I) + \frac{e\mu_{Bj}}{2qM_j} t_{ij}(\sqrt{s}) - \sum_l t_{il}(\sqrt{s}) \frac{\partial G_l(s)}{\partial \sqrt{s}} t_{lj}(M_I) \frac{e\mu_{Bl}}{2M_l} \quad (10)$$

The fact that in the amplitudes of eqs. (8-10) the strong t matrix appears sometimes with the argument M_I makes it convenient to evaluate the phase space for the cross section with $d^3q/2q$ in the CM of the K^-p system and $d^3k'/2w(k')$ in the CM of the final meson baryon system. Hence we have

$$k \cdot q = k^0 q^0 - kq \cos \theta, \quad (11)$$

$$k' \cdot q = \tilde{k}'^0 \tilde{q}^0 - \tilde{k}' \tilde{q} \cos \theta', \quad (12)$$

with \tilde{k}' , \tilde{q} the final meson and photon momenta in the final meson baryon CM frame,

$$\tilde{q} = \frac{q\sqrt{s}}{M_I}, \quad \tilde{k}' = \frac{\lambda^{1/2}(M_I^2, m_j^2, M_j^2)}{2M_I}, \quad \tilde{k}^0 = \frac{M_I^2 + m_j^2 - M_j^2}{2M_I}, \quad (13)$$

with m_j , M_j the final meson, baryon masses, θ the angle between \vec{q} and \vec{k} in the K^-p CM frame and θ' the angle between \vec{k}' and \vec{q} in the final meson baryon CM frame. By choosing an appropriate pair of orthogonal ϵ_1, ϵ_2 photon polarization vectors, also orthogonal to \vec{q} , and summing over photon and final baryon polarizations plus averaging over the initial proton polarization, we finally obtain the cross section for the process given by (σ the cross section for each i, j transition)

$$\frac{d\sigma}{dM_I d\varphi} = \frac{1}{2\pi} \frac{d\sigma}{dM_I} + \frac{d\sigma_I}{dM_I d\varphi} \cos \varphi, \quad (14)$$

with φ the azimuthal angle formed by the plane containing the \vec{k}' and \vec{q} vectors and the one containing the \vec{k} and \vec{q} vectors. The only dependence on the azimuthal angle φ comes in the $\cos \varphi$ dependence which accompanies the interference cross section, σ_I , in eq. (14), which means that both $d\sigma/dM_I$ and $d\sigma_I/dM_I d\varphi$ do not depend on the angle φ .

The expresions for $d\sigma/dM_I$ and $d\sigma_I/dM_I d\varphi$ are given by

$$\frac{d\sigma}{dM_I} = 2\pi F \{ |t^{(1E)}|^2 k^2 \sin^2 \theta + |t^{(2E)}|^2 \tilde{k}'^2 \sin^2 \theta' + 2|t_M|^2 q^2 \}, \quad (15)$$

$$\frac{d\sigma_I}{dM_I d\varphi} = F \{ -2 \text{Re}(t^{(1E)} t^{(2E)*}) k \tilde{k}' \sin \theta \sin \theta' \}, \quad (16)$$

with F an operator symbolizing

$$F \rightarrow \frac{1}{(2\pi)^4} \frac{1}{4s} \frac{M_i M_j}{\lambda^{1/2}(s, M_i^2, m_i^2)} \frac{1}{M_I} (s - M_I^2) \lambda^{1/2}(M_I^2, M_j^2, m_j^2) \\ \times \frac{1}{2} \int_{-1}^1 d\cos \theta \frac{1}{2} \int_{-1}^1 d\cos \theta'. \quad (17)$$

We show the results in figs. 2 and 3. In fig. 2 we can see the results for the cross sections in the $K^-p \rightarrow \pi^- \Sigma^+ \gamma, \pi^+ \Sigma^- \gamma, \pi^0 \Sigma^0 \gamma, \pi^0 \Lambda \gamma, K^- p \gamma$ channels.

The cross section for $K^-p \rightarrow \bar{K}^0 n \gamma$ is very small, around 0.1 mb GeV^{-1} in the range $1.44 - 1.52 \text{ GeV}$, and is not plotted in the figure. The $\Lambda(1405)$ peak appears clearly in the $\pi\Sigma$ spectrum. It is interesting to notice the difference between the cross sections for the different $\pi\Sigma$ channels. The origin of this is the same one discussed in [10] due to the different isospin combinations of the three charged states and the crossed products of the $I=1$, $I=0$ amplitudes which appear in the cross section. The $\pi^0\Sigma^0$ has no $I=1$ component and since the $I=2$ component is negligible, the $\pi^0\Sigma^0$ distribution is very similar to the $I=0$ $\Lambda(1405)$ distribution. On the other hand, the $I=1$, $I=0$ crossed products cancel in the sum of the $\pi^+\Sigma^-$, $\pi^-\Sigma^+$ distributions and the remaining sum of the squares of the $I=0$ and $I=1$ amplitudes is largely dominated by the $I=0$ contribution. Hence, both the $\pi^0\Sigma^0$ distribution or the sum of the three $\pi\Sigma$ channels have approximately the shape of the resonance. The $I=0$ contribution alone, coming from the excitation of the $\Lambda(1405)$, can be obtained using a combination of the three $\pi\Sigma$ amplitudes. Given the isospin decomposition of the $\pi\Sigma$ states, the combination that gives the $I = 0$ component is given by:

$$(t_{K^-p \rightarrow \pi^-\Sigma^+} + t_{K^-p \rightarrow \pi^+\Sigma^-} + t_{K^-p \rightarrow \pi^0\Sigma^0})/\sqrt{3}, \quad (18)$$

Hence, the $I = 0$ cross section can be obtained using eqs. (8-10) substituting t_{ij} by the combination of eq. (18).

We show the results for the pure $I=0$ excitation in fig. 2 which looks very similar to the total strength around the $\Lambda(1405)$ peak.

Below the K^-p threshold there is some strength for $I=1$, $\pi^0\Lambda$ excitation, which is also very small as shown in the figure. As a consequence of that, the sum of all channels in the $\Lambda(1405)$ region, which requires exclusively the detection of the photon, has approximately the $\Lambda(1405)$ shape and strength.

It is interesting to observe the fast rise of the cross section in the $K^-p \rightarrow K^-p\gamma$ channel, showing the Bremsstrahlung infrared divergence at large M_I (small photon momentum). The other channels also would show the infrared divergence at higher energies, when the photon momentum goes to zero. The relative larger weight of the $K^-p \rightarrow K^-p\gamma$ reaction at these energies, with respect to the other ones, is a reflection of the fact that the $K^-p \rightarrow K^-p$ cross section at values of M_I or \sqrt{s} of the order of 1500 is much bigger than the other $K^-p \rightarrow M'B'$ cross sections.

In fig. 3 we show $d\sigma_I/dM_I d\varphi$. This magnitude is interesting since it involves the $Re(t^{(1E)}t^{(2E)*})$ and hence $Re(t(M_I)t(\sqrt{s})^*)$. Since $t(\sqrt{s})$ is fixed, the interference cross section as a function of M_I shows variations of $t(M_I)$ in a different combination than the one appearing in $d\sigma/dM_I$ of fig. 2, adding complementary information on the strong scattering amplitudes, and also further testing the chiral approach used, which gives a specific weight to the different terms. The approximate different signs in the $\pi^-\Sigma^+\gamma$ and $\pi^+\Sigma^-\gamma$ channels

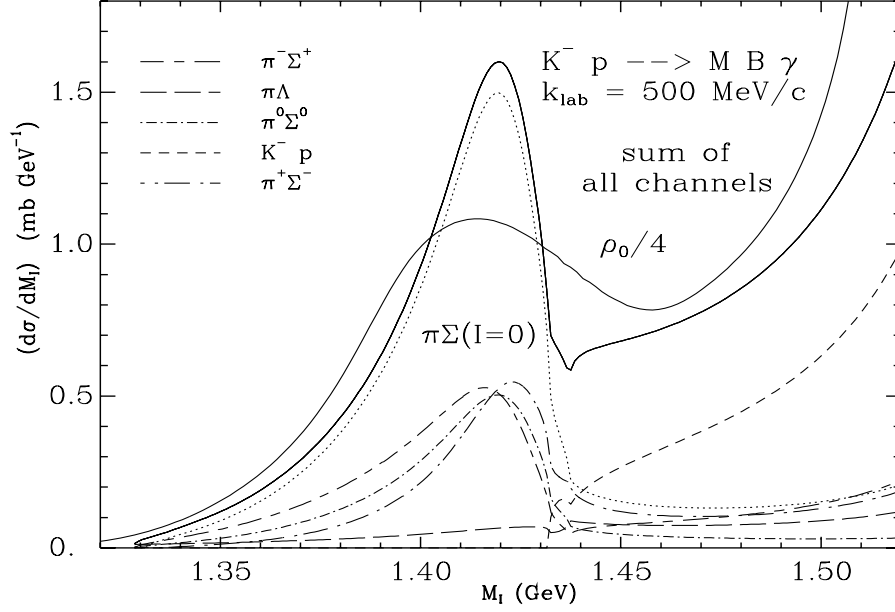


Figure 2: Mass distribution for the different channels, eq. (15). The solid line with the resonance shape is the sum of cross sections for all channels. Dotted line: pure $I = 0$ contribution from the $\Sigma\pi$ channels. The effects of the Fermi motion with ($\rho = \rho_0/4$) is shown with solid line. The labels for the other lines are shown in the figure.

observed in the figure reflect the product $Q_i Q_j$ which appears in the product of $t_{ij}^{(1E)} t_{ij}^{(2E)}$. This also tells us that the channels with neutral particles in the final state, $\bar{K}^0 n$, $\pi^0 \Lambda$, $\pi^0 \Sigma^0$, do not have any contribution to $d\sigma_I/dM_I$. This is of course another test of the approach which could be tested experimentally.

The results obtained here involve the use of the $K^- p \rightarrow MB$ interaction at higher K^- momenta than tested in [8], where K^- lab was below 200 MeV/c. The experimental cross sections extrapolate smoothly at higher energies in the range used here and the model of [8] still provides a fair description of the data [12,13,14]. Note, moreover, that the peak of $d\sigma/dM_I$ around the $\Lambda(1405)$ resonance is dominated by $t_{ij}(M_I)$ with $M_I \simeq 1400$ MeV where the model of [8] proved to be very accurate.

We have also performed calculations at lower energies of the K^- and the results are qualitatively very similar. There is, however, a lower limit to this experiment. Indeed, when the Bremsstrahlung tail of the $K^- p \rightarrow K^- p \gamma$ reaction overlaps with the $\Lambda(1405)$ signal all valuable information obtained by detecting the photon alone is lost. We have checked that this occurs for K^- lab. momenta below 200 MeV/c. However, if one detects the $\pi\Sigma$ final particles in coincidence, due to the relatively smaller weight of the cross section at high energies, one can go to smaller K^- momenta before the Bremsstrahlung

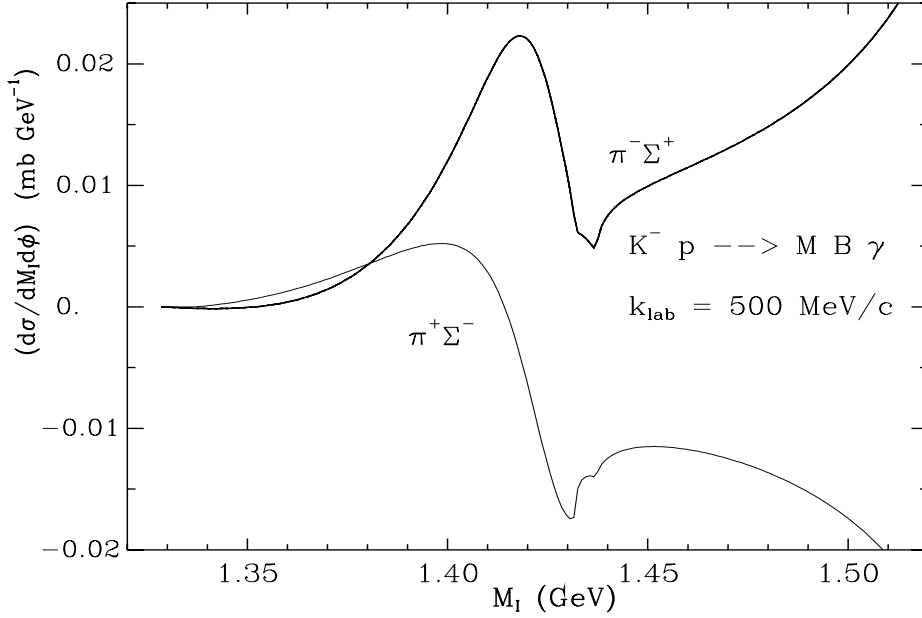


Figure 3: Double differential cross section $d\sigma_I/dM_I d\phi$ for $\Sigma^+\pi^-$ and $\Sigma^-\pi^+$.

tail also blurs the image of the $\Lambda(1405)$ resonance. We have checked that this happens below K^- lab. momenta of 150 MeV/c.

The evaluation of the corresponding reactions in nuclei would require to account for the distortion of the incoming K^- waves. In this case if one detects only the photon one has a distribution of invariant masses due to Fermi motion since now $M_I^2 = (k + p_N - q)^2$ and p_N runs over all nucleon momenta of the occupied states. We have folded our $d\sigma/dM_I$ results with the distribution of M_I coming from a Fermi sea of nucleons and show the results in fig. 2 for $\rho = \rho_0/4$, a likely effective density for this reaction, taking into account K^- distortion. We can see a widening of the $\Lambda(1405)$ distribution, with the shape only moderately changed, such that other effects from genuine changes of the $\Lambda(1405)$ properties in the medium, predicted to be quite drastic [1, 2, 3] could in principle be visible. Certainly the detailed measurement of the final meson baryon in coincidence with the photon would allow a much better determination of the $\Lambda(1405)$ properties than just the photon detection, and ultimately these exclusive measurements should also be performed.

The proposed reactions can be easily implemented at present facilities like KEK or Brookhaven. In Brookhaven some data from recent K^-p experiment with detection of photons in the final state are in the process of analysis [15]. The present results should encourage the detailed analysis of the particular channels discussed here.

Acknowledgements. We are grateful to the COE Professorship program of Monbusho, which enabled E. O. to stay at RCNP to perform the present work. One of us, J.C. Nacher would like to acknowledge the hospitality of the RCNP of the Osaka University where this work was done and support from the Ministerio de Educacion y Cultura. This work is partly supported by DGICYT contract number PB96-0753 and PB95-1249.

References

- [1] V. Koch, Phys. Lett. B337 (1994) 7
- [2] T. Waas, N. Kaiser and W. Weise, Phys. Lett B365 (1996) 12
- [3] M. Lutz, Phys. Lett. B426 (1998) 12
- [4] C. J. Batty, E. Friedman and A. Gal, Phys. Rep. 287 (1997) 385
- [5] G. E. Brown, K. Kubodera, M. Rho and V. Thorsson, Phys. Lett. B291 (1992) 355; C.H. Lee, G.E. Brown, D. P. Min and M. Rho, Nucl.Phys. A585 (1995) 401
- [6] N. Kaiser, R. Siegel and W. Weise, Nucl. Phys. A594 (1995) 325
- [7] N. Kaiser, T. Waas and W. Weise, Nucl. Phys. A612 (1997) 297
- [8] E. Oset and A. Ramos, Nucl. Phys. A635 (1998) 99
- [9] T. S. H. Lee, J. A. Oller, E. Oset and A. Ramos, Nucl. Phys. A643 (1998) 402
- [10] J. C. Nacher, E. Oset, H.Toki and A. Ramos, Phys. Lett. B in print, nucl-th/9812055
- [11] J. A. Oller, E. Oset and J. R. Peláez, Phys. Rev. Lett. 86 (1998) 3452
- [12] T. S. Mast et al., Phys. Rev. D14 (1976) 13
- [13] J. Ciborowski et al., J. Phys. G 8 (1982) 13
- [14] D. Evans et al., J. Phys. G 9 (1983) 885
- [15] R. J. Peterson, private communication.